Journal of Cerebral Blood Flow & Metabolism (2012) 32, 1909–1918

www.jcbfm.com

Effect of hypoxia and hyperoxia on cerebral blood flow, blood oxygenation, and oxidative metabolism

Feng Xu[1], Peiying Liu[1], Juan M Pascual[2], Guanghua Xiao[3] and Hanzhang Lu[1]

[1]*Advanced Imaging Research Center, University of Texas Southwestern Medical Center, Dallas, Texas, USA;* [2]*Departments of Neurology and Neurotherapeutics, Physiology and Pediatrics, University of Texas Southwestern Medical Center, Dallas, Texas, USA;* [3]*Department of Clinical Sciences, University of Texas Southwestern Medical Center, Dallas, Texas, USA*

Characterizing the effect of oxygen (O_2) modulation on the brain may provide a better understanding of several clinically relevant problems, including acute mountain sickness and hyperoxic therapy in patients with traumatic brain injury or ischemia. Quantifying the O_2 effects on brain metabolism is also critical when using this physiologic maneuver to calibrate functional magnetic resonance imaging (fMRI) signals. Although intuitively crucial, the question of whether the brain's metabolic rate depends on the amount of O_2 available has not been addressed in detail previously. This can be largely attributed to the scarcity and complexity of measurement techniques. Recently, we have developed *an* MR method that provides a noninvasive (devoid of exogenous agents), rapid (<5 minutes), and reliable (coefficient of variant, CoV <3%) measurement of the global cerebral metabolic rate of O_2 ($CMRO_2$). In the present study, we evaluated metabolic and vascular responses to manipulation of the fraction of inspired O_2 (FiO_2). Hypoxia with 14% FiO_2 was found to increase both $CMRO_2$ ($5.0 \pm 2.0\%$, $N = 16$, $P = 0.02$) and cerebral blood flow (CBF) ($9.8 \pm 2.3\%$, $P < 0.001$). However, hyperoxia decreased $CMRO_2$ by $10.3 \pm 1.5\%$ ($P < 0.001$) and $16.9 \pm 2.7\%$ ($P < 0.001$) for FiO_2 of 50% and 98%, respectively. The CBF showed minimal changes with hyperoxia. Our results suggest that modulation of inspired O_2 alters brain metabolism in a dose-dependent manner.
Journal of Cerebral Blood Flow & Metabolism (2012) **32,** 1909–1918; doi:10.1038/jcbfm.2012.93; published online 27 June 2012

Keywords: cerebral metabolic rate of oxygen; cerebral venous oxygenation; hyperoxia; hypoxia

Introduction

A tight control of cerebral perfusion and oxygen (O_2) supply is critical for brain function and health, especially because oxidative metabolism is the primary means of energy production in the brain (Magistretti and Pellerin, 1999). Characterization of the influence of O_2 availability on the brain is therefore an essential step toward a better understanding of brain energy homeostasis and also has important clinical implications. For example, acclimatization to high altitudes is triggered by hypoxia and >80% of people experience a certain degree of discomfort, including headache and shortness of breath, with a fraction of them developing acute mountain sickness that includes nausea, vomiting, fatigue, dizziness, and difficulty sleeping (Imray *et al*, 2011). However, hyperoxia has been used as a therapeutic intervention in patients with traumatic brain injury and focal ischemia (Thom, 2009). Although increased blood O_2 content is expected to enhance O_2 delivery to tissues, clinical trials of O_2 therapy have yielded mixed results, with some reporting excellent efficacy and others showing marginal benefit (Magnoni *et al*, 2003; Rockswold *et al*, 2010). One possible reason is that, while hyperoxia may benefit ischemic tissue, it may concomitantly cause oxidative stress with a potential to damage healthy brain regions. Additionally, under the assumption that changes in O_2 content do not alter brain metabolism, a hyperoxia challenge has recently been used to calibrate the Blood-Oxygenation-Level-Dependent signal in functional magnetic resonance imaging (MRI) studies (Chiarelli *et al*, 2007). Therefore, there has been a growing interest in

Correspondence: Professor H Lu, Advanced Imaging Research Center, University of Texas Southwestern Medical Center, 5323 Harry Hines Blvd., Dallas, TX 75390, USA.
E-mail: hanzhang.lu@utsouthwestern.edu
This work was supported, in part, by the National Institutes of Health (R01 MH084021, R01 NS067015, and R01 AG033106).
Received 27 January 2012; revised 22 May 2012; accepted 23 May 2012; published online 27 June 2012

understanding the effect of O_2 modulation on brain physiology.

It is well established that hyperoxia increases arterial blood O_2 content, with hypoxia having the opposite effect. Some investigators have reported a cerebral blood flow (CBF) reduction during hyperoxia, but this trend is not always observed (Bulte *et al*, 2007; Nishimura *et al*, 2007; Sicard and Duong, 2005). Even more controversial is the question whether O_2 gas modulation alters tissue metabolic rate. This uncertainty is largely due to the limited availability and sensitivity of suitable techniques to measure the cerebral metabolic rate of O_2 ($CMRO_2$) *in vivo*. Existing $CMRO_2$ techniques based on the Kety-Schmidt method or ^{15}O PET require dynamic sampling of arterial blood, which is not only invasive, but also reduces the reproducibility of the measurement (Kety and Schmidt, 1948; Mintun *et al*, 1984). Recently, our laboratory has developed an MR-based technique for the quantification of global $CMRO_2$ (Xu *et al*, 2009). This method separately measures CBF, arterial and venous oxygenation, and uses the Fick principle (i.e., calculates arteriovenous difference) to estimate $CMRO_2$. The procedure is noninvasive (i.e., no blood sampling or exogenous agent), fast (<5 minutes), and reproducible (i.e., coefficient of variation, CoV, $<3\%$) (Liu *et al*, 2012; Xu *et al*, 2009). These desirable features of the technique may allow a better detection of potential effects of O_2 modulation on $CMRO_2$.

In this study, we used the techniques described above to examine potential changes in CBF, arterial O_2 content, venous O_2 content, and $CMRO_2$ due to O_2 gas modulation. The convenience of the method allows us to investigate hypoxia (14% fraction of inspired O_2, FiO_2) and hyperoxia (administrated at two levels: 50% and 98% FiO_2) in the same study, which is different from previous studies that have focused on one challenge only. Our data suggest that both vascular and metabolic parameters of the brain are strongly dependent on the O_2 level in the inspired air.

Materials and methods

Theory for the Measurement of Global Cerebral Metabolic Rate of Oxygen

Similarly to many existing techniques, our approach to estimate $CMRO_2$ was based on the Fick principle (Kety and Schmidt, 1948). The difference between the present technique and the previous studies is that our method can measure the relevant parameters in a noninvasive manner with short and simple procedures. Brain O_2 metabolic rate can be written as:

$$CMRO_2 = CBF \cdot ([O_2]_a - [O_2]_v) \quad (1)$$

where $CMRO_2$ is in units of μmol/min, CBF is the cerebral blood flow in mL/min, $[O_2]_a$ and $[O_2]_v$ (in μmol O_2/mL blood) are O_2 contents in arterial and venous blood, respectively. Some researchers further define a term called oxygen extraction fraction, $OEF = ([O_2]_a - [O_2]_v)/[O_2]_a$. Note that, under most circumstances (e.g., room-air breathing), considerations of $[O_2]_a$ only need to focus on hemoglobin-bound O_2, as the amount dissolved in plasma is negligible ($\sim 1.8\%$ of that bound to hemoglobin). For the hyperoxia challenge used in the present study, however, the amount of dissolved O_2 is significant and should be accounted for in the calculation. Therefore, the O_2 content in the blood was calculated as:

$$[O_2]_a = Y_a \cdot C_h + p_aO_2 \cdot C_d \quad (2)$$

and

$$[O_2]_v = Y_v \cdot C_h + p_vO_2 \cdot C_d \quad (3)$$

where C_h (8.97 μmol O_2/mL blood for an Hct of 0.44, but was adjusted for each subject based on individual Hct) and C_d (0.00138 μmol O_2/mL blood/mm Hg O_2 tension) are constants associated with hemoglobin O_2-carrying capacity and blood O_2-dissolving capacity, respectively (Guyton and Hall, 2005). Y_a and Y_v are arterial and venous O_2 saturation fractions of hemoglobin (expressed in %). p_aO_2 and p_vO_2 are the O_2 tensions of the arterial and venous blood, respectively, in units of mm Hg.

Among the parameters needed to compute $CMRO_2$, the most challenging task has been the measurement of Y_v. We have recently developed and validated a technique, T_2-Relaxation-Under-Spin-Tagging (TRUST) MRI, to estimate global Y_v in the sagittal sinus (Lu and Ge, 2008; Lu *et al*, 2012). This technique was found to be highly reproducible and can be conducted within 4 minutes. Therefore, TRUST MRI was used to estimate Y_v in the present study. Once Y_v is known, p_vO_2 can also be estimated from the O_2 dissociation curve, although the dissolved O_2 in venous blood is virtually negligible compared with the hemoglobin-bound O_2. Phase-contrast (PC) MRI was used to measure CBF (Xu *et al*, 2011). Consistent with TRUST MRI, PC MRI was also performed in the sagittal sinus. Thus, the estimated $CMRO_2$ reflects the total O_2 consumed by brain tissues that are drained by the sagittal sinus. The sagittal sinus was used in our study as opposed to using jugular vein or internal carotid artery because this vessel is subject to minimal blood pulsation, which would negatively impact the image quality for both TRUST and PC MRI. Although the flow in the sagittal sinus does not provide a true whole-brain measure, the comparison of parameters across different O_2 conditions is still expected to be valid, as long as the draining path of venous blood is not altered by O_2 modulation.

For the estimation of arterial O_2 content (equation (2)), Y_a was measured with Pulse Oximeter on the index finger. For p_aO_2, some studies have assumed the value to be the same as alveolar O_2 pressure (p_AO_2), which can be determined by end-tidal (Et) O_2 measurement. In the present study, we have considered the alveolar-arterial O_2 pressure gradient ($p_{A-a\ gradient}$) and its dependence on p_AO_2 and age. Specifically, arterial O_2 pressure was estimated by $p_aO_2 = p_AO_2 - p_{A-a gradient}$, where $p_{A-a\ gradient}$ is assumed to be a linear function of p_AO_2 and age (Ayres *et al*, 1964; Stein *et al*, 1995) (see Supplementary text).

Participants

The study was approved by the Institutional Review Board of the University of Texas Southwestern Medical Center. Sixteen subjects (26 ± 4 years old, nine males and seven females) were recruited. The participants did not report pulmonary, respiratory, neurologic, or psychiatric disorders according to self-completed questionnaires. None of the participants were smokers or had asthma. The subjects gave informed written consent before participating in the study.

Oxygen Modulation

Modulation of O_2 content in the inspired air was achieved using a custom-made breathing apparatus (Xu *et al*, 2011; Yezhuvath *et al*, 2009). Briefly, after lying on the magnet table, the subject was fitted with a nose clip and a mouthpiece so that s/he could breathe through the mouth only. The mouthpiece was connected to a three-way valve, which delivers either room air (21% FiO_2) or a special gas mixture contained in a Douglas bag. Three Douglas bags containing different gas mixtures were prepared: (1) 14% O_2 and 76% N_2 (hypoxia); (2) 50% O_2, 1% CO_2, and 49% N_2 (50% hyperoxia); and (3) 98% O_2 and 2% CO_2 (98% hyperoxia). These bags sequentially connected to the valve, thereby switching the inspired air. Note that a small amount of CO_2 was intentionally added to the hyperoxia gas mixture because hyperoxia tends to cause the subject to hyperventilate, resulting in an unwanted physiologic change of reduced arterial CO_2 level, which may have additional effects on CBF and $CMRO_2$ (Cohen *et al*, 2002). We therefore added CO_2 to partially offset this side effect. Similar strategies have been used in previous reports in the literature (see also Discussion) (Floyd *et al*, 2003).

The study paradigm consisted of a continuous, 50-minute session in which the subject breathed the above-mentioned gas mixtures in the following order: room air (21% FiO_2) for 8 minutes, 14% FiO_2 for 18 minutes, 50% FiO_2 for 15 minutes, and 98% FiO_2 for 12 minutes (see color coding in Figure 1). The duration of each breathing period was determined based on the time needed to reach a new steady state after switching the gas (calibrated from tests conducted outside the MRI). For example, it takes more time for the 14% FiO_2 condition to reach a steady state, therefore the administration for this gas mixture was the longest.

During the experiment, the participant was instructed to keep still and maintain a uniform breathing pattern. To prevent drowsiness, an individually selected movie was shown to the participant via a back-projection video system (typically used for functional MRI fMRI) throughout the session. The rationale for this intervention was to prevent potential effects of sleep and drowsiness on brain CBF and metabolism (Braun *et al*, 1997; Nofzinger *et al*, 2002). Continuous physiologic recordings were obtained for end-tidal (Et) CO_2 (Capnograph; Novametrix Medical System, Wallingford, CT, USA), EtO_2 (Analox Sensor Technology, Stokesley, North Yorkshire, UK), Y_a (MEDRAD, Pittsburgh, PA, USA), and heart rate (MEDRAD). After the MRI scans were completed and the subject exited the scanner room, a blood sampling with a potassium ethylenediaminetetraacetic acid-coated 10 mL lavender tube was conducted on the basilic vein of the arm and Hct was measured with a centrifuge (Hemata STAT II, Separation Technology, Inc., Altamonte Springs, FL, USA). Determination of Hct is needed to obtain an accurate blood oxygenation estimation from the MRI measure of T_2 (Lu *et al*, 2012).

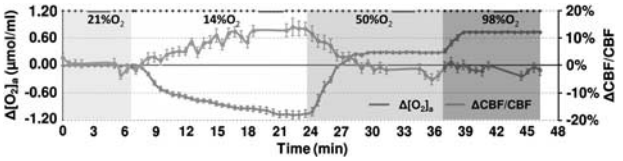

Figure 1 Illustration of experimental paradigm and time courses of arterial oxygen content, $[O_2]_a$, and cerebral blood flow (CBF). During the session, the subject breathed 21%, 14%, 50%, and 98% fraction of inspired O_2 (FiO_2) for 8, 18, 15, and 12 minutes, respectively, and these are denoted by different colors in the plot. The duration of each condition was preset based on the time needed to reach a new steady state that was determined from several testing experiments. Magnetic resonance imaging (MRI) data acquisitions were performed throughout the session and the type of pulse sequence performed is denoted as dots or bars at the top of the plot, where each dot indicates a 0.5-minute phase-contrast MRI and each bar indicates a 3.2-minute T_2-Relaxation-Under-Spin-Tagging (TRUST) MRI. Due to the large number and high density of the phase-contrast scans, the data allowed the assessment of time course of CBF changes (blue curve) during the experiment (the gap in the curve is due to the TRUST scan). For comparison, $[O_2]_a$ (accounting for both hemoglobin-bound and dissolved O_2) time course is also display (red curve). The color reproduction of this figure is available at the *Journal of Cerebral Blood Flow and Metabolism* journal online.

Magnetic Resonance Imaging Experiments

The MRI scans were performed on a 3-Tesla system (Philips Medical Systems, Best, The Netherlands). Two sequences, TRUST MRI and PC MRI, were performed multiple times during the entire session and their timing is shown in Figure 1 (bars and dots, respectively, at the top of the figure). The TRUST MRI (duration 3.2 minutes) was performed four times during the steady states of the four O_2 conditions. The PC MRI (duration 0.5 minutes) was performed during the rest of the time. In principle, only four PC scans, one for each O_2 condition under steady state, were needed for the study. We, however, acquired PC MRI continuously throughout the session (except when TRUST is being acquired) because (1) the PC scan is very short in duration and a continuous acquisition would allow us to evaluate CBF changes in transitional states while FiO_2 changes; (2) multiple PC scans acquired before and after the TRUST scan would allow us to interpolate the CBF values to better match the timing of Y_v values from TRUST MRI.

The TRUST technique uses the spin labeling principle to isolate pure venous blood signals and measures T_2 value of the blood, followed by conversion of T_2 to O_2 saturation

fraction with a calibration plot (Lu and Ge, 2008). Sequence parameters of TRUST MRI were single slice intersecting superior sagittal sinus at ~10 mm above the sinus congruence, voxel size = $3.44 \times 3.44 \times 5\,mm^3$, repetition time = 8,000 ms, inversion time = 1,200 ms, τ_{CPMG} T_2 preparation with MLEV16 phase cycling, $\tau_{CPMG} = 10$ ms, four effective echo time (TEs) = 0, 40, 80, and 160 ms, scan duration = 3.2 minutes.

Quantitative PC MRI measures blood flow using magnetic field gradients (Xu *et al*, 2009). The phase of the magnetization is associated with the velocity value. The sequence parameters of PC MRI were single slice at the same position as TRUST MRI, voxel size = $0.45 \times 0.45 \times 5\,mm^3$, field-of-view = $230 \times 230 \times 5\,mm^3$, maximum velocity = 80 cm/s, number of averages = 4, duration = 30 seconds.

Data Processing

The data processing procedures for TRUST MRI and PC MRI were based on algorithms described previously (Lu and Ge, 2008; Xu *et al*, 2009; see Supplementary text). For each FiO_2 condition, Y_v and CBF were obtained. The Y_v value was estimated from the corresponding TRUST scan. The CBF was obtained from the average of four PC scans before and four PC scans after TRUST MRI. The averaging improves data stability and also better matches the physiologic states between PC and TRUST acquisition periods (in case there is a physiologic drift during these periods).

Physiologic recordings of Y_a and EtO_2 were used to obtain other parameters needed for $CMRO_2$ calculation. The recorded values during the corresponding MRI acquisition period were averaged to obtain the final value used in the calculation. The $CMRO_2$ under each O_2 condition was estimated using equations (1–3). Using room-air condition as a reference, changes in physiologic parameters due to the special gas mixture were calculated.

Statistical Analysis

Statistical analyses were performed to examine whether each of the gas mixtures (i.e., $FiO_2 = 14\%$, 50%, and 98%, respectively) resulted in an alteration in brain metabolic and vascular parameters. Specifically, a one sample Student's *t*-test was used to evaluate whether ΔCBF/CBF and $\Delta CMRO_2/CMRO_2$ were significantly different from zero. We used fractional changes as opposed to absolute changes because the original experimental measures are affected by the brain size of the individual and the use of fractional changes provides a normalized measure. A $P < 0.05$ is considered a significant effect.

Because hyperoxia and hypoxia may also change CO_2 content in the blood ($[CO_2]_a$) due to hyperventilation, the observed physiologic changes may be partially attributed to a CO_2 effect. We therefore corrected for the CO_2 effect and reanalyzed the data using the corrected values. The corrections were made by calculating:

$$\frac{\Delta CMRO_2}{CMRO_2}|_{corrected} = \frac{\Delta CMRO_2}{CMRO_2}|_{uncorrected} - f(\Delta[CO_2]_a) \quad (4)$$

and

$$\frac{\Delta CBF}{CBF}|_{corrected} = \frac{\Delta CBF}{CBF}|_{uncorrected} - g(\Delta[CO_2]_a) \quad (5)$$

where $\Delta[CO_2]_a$ is the alteration in CO_2 content during the O_2 challenge, the functions $f(\cdot)$ and $g(\cdot)$ represent the dependence of $\Delta CMRO_2/CMRO_2$ and ΔCBF/CBF on $\Delta[CO_2]_a$, respectively. $f(\cdot)$ and $g(\cdot)$ were assumed to be a second-order polynomial (consistent with the expression for O_2 dependence as described later):

$$f(\Delta[CO_2]_a) = m \cdot \Delta[CO_2]_a + n \cdot \Delta[CO_2]_a^2 \quad (6)$$

and

$$g(\Delta[CO_2]_a) = p \cdot \Delta[CO_2]_a + q \cdot \Delta[CO_2]_a^2 \quad (7)$$

The coefficients in equations (6) and (7) were estimated by fitting of experimental data from an earlier report (Xu *et al*, 2011), in which $[CO_2]_a$ was specifically maneuvered to examine its effect on $CMRO_2$. Note that $[CO_2]_a$ is not only dependent on $EtCO_2$, but also on arterial O_2 saturation level (Y_a) because of the Haldane effect (Loeppky *et al*, 1983). In this study, the calculation of $[CO_2]_a$ accounted for both factors (see Supplementary text).

Using equations (6) and (7) and data in Xu *et al* (2011), the coefficients, *m*, *n*, *p*, and *q*, were found to be −0.006, −0.029, 0.068, and 0.098, respectively. To further examine error propagation from these coefficient values to the results of the present study, we conducted Monte Carlo simulations based on covariance matrices of *m*, *n*, *p*, and *q* (see Supplementary text).

Because $CMRO_2$ and CBF alterations during O_2 modulation are most likely mediated by O_2 content in the arterial blood and that different individuals may manifest different responses in arterial O_2 even given identical FiO_2, we conducted further analyses to directly examine the dependence of $\Delta CMRO_2/CMRO_2$ and ΔCBF/CBF on $\Delta[O_2]_a$. A mixed effect regression model (R software, Wirtschaftsuniversität Wien Vienna University, Austria) was used in which $\Delta[O_2]_a$ was the independent variable and had three observations for each subject, and the respective physiologic parameter was used as the dependent variable. Second-order polynomials, i.e.,

$$\frac{\Delta CMRO_2}{CMRO_2} = a \cdot \Delta[O_2]_a + b \cdot \Delta[O_2]_a^2 \quad (8)$$

and

$$\frac{\Delta CBF}{CBF} = c \cdot \Delta[O_2]_a + d \cdot \Delta[O_2]_a^2 \quad (9)$$

were used for the model as the data (see Results and Discussion) suggested that the second-order model provides a better fitting than the linear model, as determined by a hierarchical regression analysis. Error propagation from the CO_2 coefficients to O_2 coefficients was again assessed by Monte Carlo simulations (see Supplementary text).

Results

All subjects were able to complete the breathing tasks without discomfort. Table 1 summarizes the vital signs during each breathing condition. Compared with room air, hyperoxia increased EtO_2, Y_v, $[O_2]_a$, and $[O_2]_v$, while hypoxia decreased them ($P<0.001$ for all tests), as expected. Y_a was reduced by hypoxia ($P<0.001$), but was minimally affected by hyperoxia as the values were already close to unity at room-air breathing. Both hyperoxia and hypoxia reduced $EtCO_2$ ($P<0.001$) (possibly due to hyperventilation), although the absolute values of the $EtCO_2$ changes were small (1 to 3 mm Hg). Hypoxia appeared to also increase the heart rate ($P<0.001$), similarly to previous reports (Tuunanen and Kauppinen, 2006).

Figure 2 shows representative imaging data for the measurements of venous oxygenation (panels A to C) and CBF (panel D). Figure 2A illustrates control, tagged, and difference images from TRUST MRI. The difference signals were then fitted as a function of effective TE to obtain the decay time constant T_2 (Figure 2B). Blood T_2 values are then converted to oxygenation using a hematocrit-specific calibration plot (Figure 2C). Figure 2D shows flow velocity maps obtained from PC MRI. Darker color indicates faster flow velocity at head-to-foot direction.

Table 2 summarizes the $CMRO_2$ and CBF values under different O_2 conditions before and after correction of CO_2 effects. The raw data (i.e., before correcting for CO_2 effects) revealed that inhalation of 14% O_2 significantly increased $CMRO_2$ ($N=16$, $P=0.02$) and CBF ($P=0.001$), while 50% FiO_2 decreased them ($P<0.001$ and $P=0.01$ for $CMRO_2$ and CBF, respectively). Inhalation of 98% O_2 decreased them further. After correction for CO_2 effects, the results became slightly different (Table 2). Figure 3

Table 1 Vital signs under various FiO_2 conditions ($N=16$, mean ± s.e.)

FiO_2	EtO_2 (mm Hg)	Y_a (%)	Y_v (%)	$[O_2]_a$ (μmol/mL)	$[O_2]_v$ (μmol/mL)	$[O_2]_a$-$[O_2]_v$ (μmol/mL)	$EtCO_2$ (mm Hg)	$[CO_2]_a$ (μmol/mL)	HR (beats/min)	BR (breaths/min)
21%	121.3 ± 0.8	98 ± 0.1	65.1 ± 1.4	8.6 ± 0.2	5.6 ± 0.2	3.0 ± 0.1	42.4 ± 0.9	19.7 ± 0.2	65 ± 3	13 ± 1
14%	67.4 ± 0.7	87 ± 0.9	54.6 ± 1.1	7.5 ± 0.2	4.7 ± 0.1	2.8 ± 0.1	41.2 ± 0.8	19.7 ± 0.2	75 ± 3	14 ± 1
50%	336.5 ± 0.9	99 ± 0.03	70.5 ± 1.5	8.9 ± 0.2	6.1 ± 0.2	2.8 ± 0.1	41.2 ± 0.8	19.4 ± 0.2	62 ± 3	15 ± 1
98%	692.9 ± 2.1	99 ± 0.05	75.7 ± 1.9	9.3 ± 0.1	6.5 ± 0.3	2.8 ± 0.1	39.2 ± 0.8	18.9 ± 0.2	64 ± 3	15 ± 1

EtO_2/CO_2, end-tidal O_2/CO_2; $Y_{a/v}$, arterial/venous blood oxygenation; $[O_2]_{a/v}$, arterial/venous blood O_2 content; HR, heart rate; BR, breathing rate; FiO_2, fraction of inspired O_2.

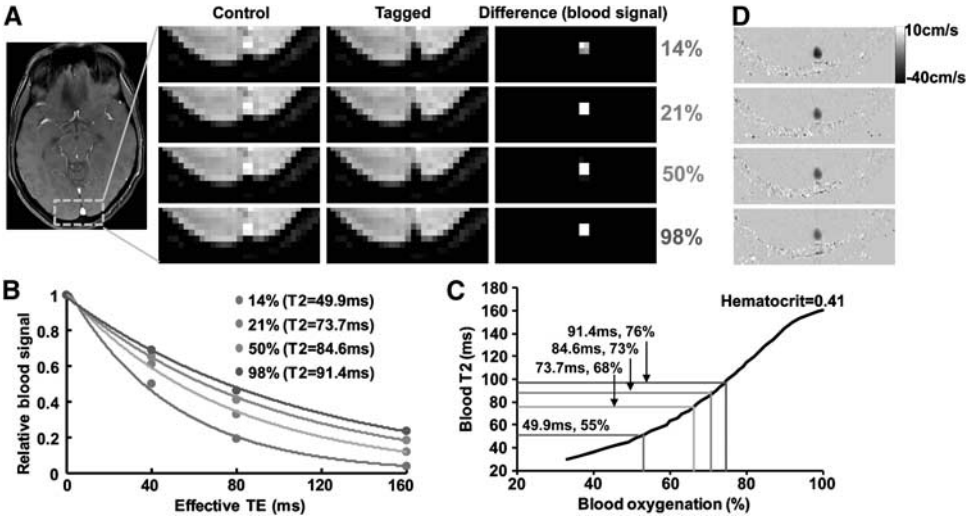

Figure 2 Representative magnetic resonance imaging (MRI) data obtained in the experiment. (**A**) Typical T_2-Relaxation-Under-Spin-Tagging (TRUST) MRI data under different fraction of inspired O_2 (FiO_2) conditions. Under each condition, control and tagged types of images were acquired, the subtraction of which yielded pure blood signal. In this study, the venous signal in the primary draining vein, sagittal sinus (center of the yellow box), was used for quantitative analysis. (**B**) In the TRUST sequence, the signal was acquired at different effective echo time (TE) values. Thus, the fitting of the signal as a function of effective TE can provide an estimation of blood T_2. The legend shows that T_2 increases with FiO_2 value. (**C**) Using a calibration plot established previously, the blood T_2 can be converted to blood oxygenation, given the subject's hematocrit value. (**D**) Representative phase-contrast MR images under different FiO_2 conditions. In these images, head-to-foot flow direction is displayed as black color. Thus, the darker the voxel appears, the higher the flow velocity is. The color reproduction of this figure is available at the *Journal of Cerebral Blood Flow and Metabolism* journal online.

Table 2 CBF and $CMRO_2$ values as a function of FiO_2 before and after correction for CO_2 effect

FiO_2	$CMRO_2$(μmol/mL)		CBF (mL/min)	
	Before correction	*After correction*	*Before correction*	*After correction*
21% O_2	1,112.7 ± 22.5	1,112.7 ± 22.5	384.7 ± 17.3	384.7 ± 17.3
14% O_2	1,166.4 ± 28.8	1,166.8 ± 29.1	421.8 ± 19.3	421.4 ± 19.0
50% O_2	1003.7 ± 27.7	997.8 ± 27.0	365.6 ± 14.3	377.3 ± 15.0
98% O_2	940.2 ± 36.0	915.2 ± 33.6	344.6 ± 13.1	387.7 ± 14.9

O_2, oxygen; CBF, cerebral blood flow; $CMRO_2$, cerebral metabolic rate of O_2; FiO_2, fraction of inspired O_2.

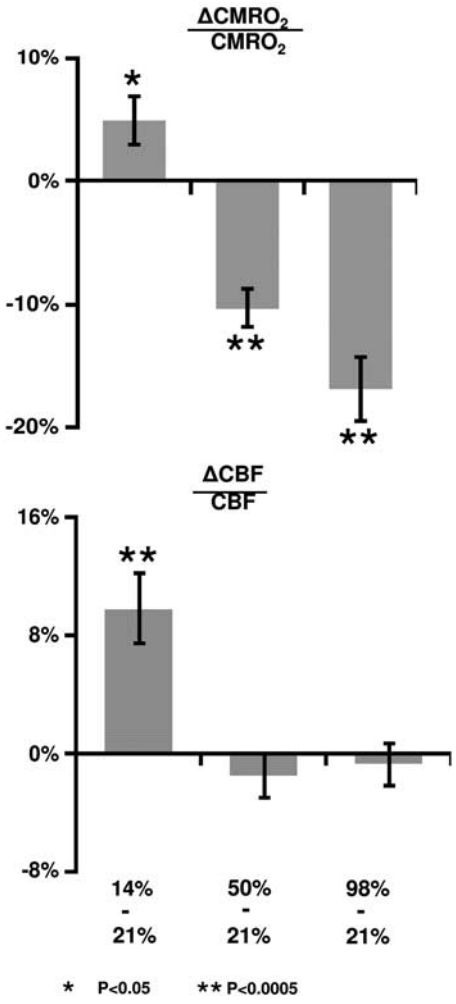

Figure 3 Percent changes in cerebral metabolic rate of oxygen ($CMRO_2$) and cerebral blood flow (CBF) due to fraction of inspired O_2 (FiO_2) modulation. The changes were calculated based on comparisons between the special gas mixture and room air.

shows the $CMRO_2$ and CBF changes due to hypoxia and hyperoxia based on the CO_2 effect corrected data. Hypoxia increased both $CMRO_2$ (5.0 ± 2.0%, mean ± s.e., $P = 0.02$) and CBF (9.8 ± 2.3%, $P < 0.001$). However, hyperoxia did not alter CBF, but decreased $CMRO_2$ by 10.3 ± 1.5% ($P < 0.001$) and 16.9 ± 2.7% ($P < 0.001$) for FiO_2 of 50% and 98%, respectively.

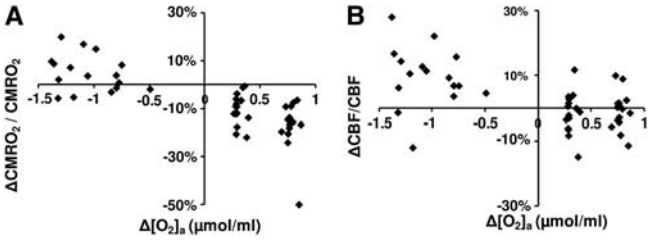

Figure 4 Scatter plots comparing (**A**) $\Delta CMRO_2/CMRO_2$ with $\Delta[O_2]_a$ and (**B**) ΔCBF/CBF to $\Delta[O_2]_a$. Even given the same fraction of inspired O_2 (FiO_2) gas type, different individuals manifest slightly different $\Delta[O_2]_a$ values. Thus, the use of $\Delta[O_2]_a$ allows a more accurate assessment of the dependence of brain physiology on O_2 content. CBF, cerebral blood flow; $CMRO_2$, cerebral metabolic rate of oxygen.

Dynamic acquisitions of CBF MRI allowed us to obtain a time course of this parameter and the group-averaged data (corrected for CO_2 effect) are shown in Figure 1. Consistent with the quantitative results described above, the time course revealed a gradual CBF increase during the hypoxia period, but did not significantly change during hyperoxia.

A scatter plot of corrected $\Delta CMRO_2/CMRO_2$ versus $\Delta[O_2]_a$ is shown in Figure 4A. Regression analyses revealed a significant inverse relationship between these parameters ($P < 0.001$). A second-order polynomial was found to provide a better fitting of the data compared with a first-order model (second-order versus first-order comparison $P = 0.007$). The coefficient values and their confidence intervals are listed in Table 3. A third-order model was not better than the second-order model ($P = 0.89$). Figure 4B shows a scatter plot of corrected ΔCBF/CBF versus $\Delta[O_2]_a$. The data were well fitted by a regression model, with a second-order polynomial (Table 3) again providing a better fitting ($P = 0.025$) than a linear model. A third-order model was not better than the second order ($P = 0.26$).

Discussion

To the best of our knowledge, the present study is the first to concomitantly examine the influence of hypoxia and hyperoxia on brain O_2 metabolism in conscious humans. Our data suggested that hypoxia by inhalation of 14% O_2 increased $CMRO_2$, while hyperoxia by inhalation of 50% O_2 decreased $CMRO_2$. Further reduction in $CMRO_2$ was observed when increasing the FiO_2 to 98%. The present study also revealed that CBF was augmented by hypoxia, but was unchanged during hyperoxia.

Physiological Considerations

The influence of FiO_2 on brain metabolism has previously been investigated by a limited number of

Table 3 Coefficient values and their confidence intervals describing the dependence of $CMRO_2$ and CBF on $\Delta[O_2]_a$

	$\frac{\Delta CMRO_2}{CMRO_2} = a \cdot \Delta[O_2]_a + b \cdot \Delta[O_2]_a^2$		$\frac{\Delta CBF}{CBF} = c \cdot \Delta[O_2]_a + d \cdot \Delta[O_2]_a^2$	
Coefficient	*a*	*b*	*c*	*d*
Value	−0.15	−0.056	−0.046	0.038
95% CILL	−0.17	−0.095	−0.073	0.0052
95% CIUL	−0.12	−0.017	−0.019	0.071
P value	<0.001	0.007	0.002	0.025

CILL, confident interval lower limit; CIUL, confident interval upper limit; CBF, cerebral blood flow; $CMRO_2$, cerebral metabolic rate of O_2.

studies (the relatively small number is mainly due to technical complexity and availability of $CMRO_2$ measurement). The results were heterogeneous. A few studies reported findings similar to ours. For example, Richards *et al*, (2007) measured O_2 metabolism in beagles using a ^{13}C NMR method and found that hyperoxia treatment after ischemia reduced O_2 metabolism. Working with a rat model, Harik *et al*, (1995) measured glucose metabolism with a 2-deoxyglucose method and observed that hypoxia with 10% FiO_2 increased glucose metabolism by 10% to 40%. A preliminary report by Smith *et al*, (2011) also noted an elevated $CMRO_2$ during hypoxia in humans, using techniques similar to ours. A few other reports contradict our findings. Comparing high altitude (~11% FiO_2) to sea level, Moller *et al*, (2002) found no changes in $CMRO_2$ or CBF using a ^{133}Xe technique. Rockswold *et al*, (2010) studied O_2 metabolism in brain injury patients using a nitrous oxide technique and found that hyperoxia increased $CMRO_2$, but Diringer *et al*, (2007) found no $CMRO_2$ changes. Several reasons may have contributed to these discrepancies, including different species, experimental conditions as well as pathological effects (Diringer *et al*, 2007; Maandag *et al*, 2007; Moller *et al*, 2002; Rockswold *et al*, 2010). Collectively, these factors make a direct comparison virtually impossible. The techniques used in the previous studies required the injection of an exogenous tracer as well as continuous sampling of arterial and venous blood, all of which may present physiologic stress and alteration to the brain (Moller *et al*, 2002; Rockswold *et al*, 2010). The present study capitalized on a recently developed global $CMRO_2$ technique that was fast, reliable, and noninvasive (Xu *et al*, 2009). The relatively simple procedure afforded by this technique allowed us to apply both hypoxia and hyperoxia in the same session.

If our findings of $CMRO_2$ alteration reflect a corresponding change in neural activity, what could the possible mechanisms be? Hyperoxia has been long known to increase the generation of reactive oxygen species (Jamieson *et al*, 1986), which could cause oxidative damage to lipids and proteins (Tatarkova *et al*, 2011). Reactive oxygen species may in turn decrease enzymatic activities in aerobic metabolism pathways via inhibition of pyruvate dehydrogenase (Bogaert *et al*, 1994), a critical enzyme in transforming pyruvate into acetyl-CoA for the citric acid cycle. A few reports have also suggested that hyperoxia may decrease gene expression associated with neurotransmitter transport and transmission (Chen *et al*, 2009). Finally, studies have shown that long-duration hyperoxia (>1 hour) may lead to apoptosis by modification of antiapoptotic proteins (Brutus *et al*, 2009; Mudduluru *et al*, 2010). This evidence suggests that hyperoxia may suppress neural activity and therefore $CMRO_2$ via several O_2 toxicity-related pathways. The effect of hypoxia on $CMRO_2$ supposedly operates via mechanisms opposite to that of hyperoxia. Previous studies have suggested that hypoxia with 8% FiO_2 can cause a 57% increase in the rate of glycolysis and a threefold increase in the activity of cytochrome oxidase, an enzyme in the mitochondrial electron transport chain (Hamberger and Hyden, 1963). Furthermore, these changes were primarily located in neurons but not in glial cells (Hamberger and Hyden, 1963), suggesting an enhancement in neuronal activity during hypoxia.

Compared with $CMRO_2$, more literature is available on the effect of FiO_2 on CBF. Our observation of an increased CBF during hypoxia is consistent with earlier reports (Noth *et al*, 2008). For a hyperoxia challenge, we observed a $11.7 \pm 1.3\%$ CBF reduction in the presence of a 3.2 ± 0.4 mm Hg $EtCO_2$ decrease (for a 98% FiO_2). Given the modulation effect of CO_2 on CBF, it seems that the observed CBF change is predominantly attributed to a CO_2 effect rather than to an O_2 effect. Indeed, after correcting for the CO_2 effect, no apparent effect of O_2 was detected. Similar findings have been reported in the literature. For example, observed a 16% CBF reduction in the context of a 3 mm Hg $EtCO_2$ decrease comparing 100% FiO_2 with 21% FiO_2. However, a few reports in the literature showed some discrepancy from our results. used Arterial-Spin-Labeling MRI to evaluate the effect of hyperoxia on CBF and noted a 28% reduction in hyperoxia. One possible explanation for this finding is that arterial T_1 is also affected by hyperoxia. Specifically, hyperoxygenation causes a blood T_1 reduction by ~30% (Silvennoinen *et al*, 2003), which would result in a lower Arterial-Spin-Labeling signal even if the CBF value did not change. The PC MRI technique used in the present study does not depend on arterial T_1. used a Dynamic-Susceptibility-Contrast MRI technique and observed a regional CBF reduction in some, but not

all brain regions. Interestingly, the authors also conducted a large vessel-based measure using transcranial Doppler techniques, and found no CBF reduction, which is similar to our large-vessel measure with PC MRI.

Technical Considerations

The $CMRO_2$ method used in the present study was based on the Fick principle of arteriovenous differences in O_2 contents, in which the contributing parameters were measured individually (Xu *et al*, 2009). This principle has been known for decades, but its implementation in humans has been challenging. The main technical obstacle was the difficulty of estimating venous oxygenation quantitatively and reliably. With a recent TRUST MRI technique that was developed by our laboratory, the quantification of global venous oxygenation becomes more feasible (Lu and Ge, 2008). The TRUST technique has been validated in humans against a gold-standard pulse oximetry method (Lu *et al*, 2012). Another parameter in the Fick principle, CBF, was determined with a PC MRI technique. Compared with other CBF quantification techniques such as Arterial-Spin-Labeling MRI, the PC technique is not affected by arterial transit time, blood and tissue T_1 values, and is thus expected to provide a more accurate estimation of global CBF. Phase-contrast MRI has previously been validated under both *in-vitro* and *in-vivo* conditions (Bakker *et al*, 1999; Evans *et al*, 1993; Zananiri *et al*, 1991).

Since changes in alertness during the experiment may alter $CMRO_2$ (in addition to any O_2 effect) (Braun *et al*, 1997; Nofzinger *et al*, 2002), the subjects of this study were allowed to view a movie while in the scanner. The postMRI questionnaire confirmed that all subjects remained awake during the entire session. Another physiologic variable that was controlled was the end-tidal CO_2 level. The subjects were instructed to maintain a uniform breathing pattern throughout the experiment. However, due to O_2 effects on chemoreceptors in the brain (Dean *et al*, 2004), hyperventilation is known to occur during a hyperoxia challenge, which results in a reduced $EtCO_2$ as documented by a number of studies in the literature (Baddeley *et al*, 2000; Dean *et al*, 2004; Guyton and Hall, 2005). To minimize CO_2 changes during the hyperoxia challenge, we added a small amount of CO_2 to the hyperoxic air (1% and 2% CO_2 to FiO_2 50% and 98%, respectively). This procedure was found to be partially effective, especially for the 50% FiO_2 condition where the $EtCO_2$ change is now only $\sim$1 mm Hg (Table 1). To further minimize the influence of CO_2 change on our data interpretation, a correction was made based on the literature reports of $CMRO_2$ and CBF dependence on $[CO_2]_a$, as described in the Materials and methods. Because the correction curve itself may contain experimental errors, we conducted an error propagation analysis using Monte Carlo simulations (see Supplementary text). We found that the coefficients associated with the $CMRO_2$ and O_2 relationship were only modestly affected by the correction curve. Within our simulations (1,000 m and n sets), the coefficients a and b in equation (8) were -0.14 ± 0.019 (mean $\pm$ s.d.) and -0.055 ± 0.011, respectively, both of which were significantly less than zero ($P < 0.001$).

In the estimation of venous O_2 pressure (thereby the amount of dissolved O_2), we did not account for the pH influence on the O_2 dissociation curve (known as the Bohr Effect). Although changes in $[CO_2]_a$ may alter pH, thereby shifting the curve, the impact of this effect on our $CMRO_2$ estimation is expected to be minimal as the dissolved O_2 in the venous blood is negligible compared with hemoglobin-bound O_2.

Implications for Calibrated Functional Magnetic Resonance Imaging

It has recently been proposed that hyperoxia can be used as a physiologic challenge in calibrated fMRI (Chiarelli *et al*, 2007). The previous study has assumed that hyperoxia does not alter $CMRO_2$. In the context of a $CMRO_2$ reduction as suggested in the present study, the theoretical framework described in Chiarelli *et al* remains valid. However, the experimental implementation should be adjusted slightly. Specifically, one could consider adding a TRUST scan during both normoxia and hyperoxia periods (which gives $[dHb]_{v0}$ and $[dHb]_v$) and then estimating M using equation (3b) in Chiarelli *et al* (2007).

One may also speculate the use of hypoxia for calibrated fMRI. However, since arterial blood also contains deoxyhemoglobin, the model becomes considerably more complicated due to the need to account for arterial oxygenation and arterial blood volume. More work is therefore needed to explore the feasibility of hypoxia for fMRI calibration.

Limitations of the Study

The findings from the present study should be interpreted in view of several limitations. One is that the technique used in the present study could only measure global $CMRO_2$, but no regional values were obtained. Therefore, while the data suggested a clear effect of O_2 on brain metabolism, it was not possible to evaluate potential regional heterogeneity of this effect or whether certain brain regions are more sensitive to O_2 challenge. Another limitation is that the study has only included young, healthy control subjects, thus the results may not be applicable to elders or patients with traumatic brain injury or brain ischemia. Finally, despite our efforts to control and correct for CO_2 effects, it would have been ideal to use a CO_2 clamping method (Wise *et al*, 2007) in the experiments. The correction approach used in the present study is based on the literature

results on the influence of CO_2 on $CMRO_2$ and CBF. It should be noted, however, that these literature data were measured under normoxia conditions. Under hyperoxia or hypoxia conditions, the relationship between $CMRO_2$/CBF and CO_2 may be different (i.e., there could be an interaction term between O_2 and CO_2 effects). There is some evidence suggesting that the interaction term is negligible for CBF (Floyd *et al*, 2003). However, future studies are needed to examine the interaction effect on $CMRO_2$.

Conclusions

The present study suggests that, aside from the expected effect on blood O_2 saturation, hypoxia enhanced brain metabolic rate while hyperoxia suppressed it. Additionally, CBF was increased in hypoxia but showed no apparent changes during hyperoxia.

Acknowledgements

The authors would like to express gratitude to Yamei Cheng for assistance with the experiments and to Dr A. Dean Sherry for helpful discussions. The authors are also grateful to Dr Janet Jerrow for scientific editing of the manuscript.

Disclosure/conflict of interest

The authors declare no conflict of interest.

References

Ayres SM, Criscitiello A, Grabovsky E (1964) Components of alveolar-arterial O2 difference in normal man. *J Appl Physiol* 19:43–7

Baddeley H, Brodrick PM, Taylor NJ, Abdelatti MO, Jordan LC, Vasudevan AS, Phillips H, Saunders MI, Hoskin PJ (2000) Gas exchange parameters in radiotherapy patients during breathing of 2%, 3.5% and 5% carbogen gas mixtures. *Br J Radiol* 73:1100–4

Bakker CJ, Hoogeveen RM, Viergever MA (1999) Construction of a protocol for measuring blood flow by two-dimensional phase-contrast MRA. *J Magn Reson Imaging* 9:119–27

Bogaert YE, Rosenthal RE, Fiskum G (1994) Postischemic inhibition of cerebral cortex pyruvate dehydrogenase. *Free Radic Biol Med* 16:811–20

Braun AR, Balkin TJ, Wesenten NJ, Carson RE, Varga M, Baldwin P, Selbie S, Belenky G, Herscovitch P (1997) Regional cerebral blood flow throughout the sleep-wake cycle. An H2(15)O PET study. *Brain* 120(Pt 7):1173–97

Brutus NA, Hanley S, Ashraf QM, Mishra OP, Delivoria-Papadopoulos M (2009) Effect of hyperoxia on serine phosphorylation of apoptotic proteins in mitochondrial membranes of the cerebral cortex of newborn piglets. *Neurochem Res* 34:1219–25

Bulte DP, Chiarelli PA, Wise RG, Jezzard P (2007) Cerebral perfusion response to hyperoxia. *J Cereb Blood Flow Metab* 27:69–75

Chen Y, Nadi NS, Chavko M, Auker CR, McCarron RM (2009) Microarray analysis of gene expression in rat cortical neurons exposed to hyperbaric air and oxygen. *Neurochem Res* 34:1047–56

Chiarelli PA, Bulte DP, Wise R, Gallichan D, Jezzard P (2007) A calibration method for quantitative BOLD fMRI based on hyperoxia. *Neuroimage* 37:808–20

Cohen ER, Ugurbil K, Kim SG (2002) Effect of basal conditions on the magnitude and dynamics of the blood oxygenation level-dependent fMRI response. *J Cereb Blood Flow Metab* 22:1042–53

Dean JB, Mulkey DK, Henderson 3rd RA, Potter SJ, Putnam RW (2004) Hyperoxia, reactive oxygen species, and hyperventilation: oxygen sensitivity of brain stem neurons. *J Appl Physiol* 96:784–91

Diringer MN, Aiyagari V, Zazulia AR, Videen TO, Powers WJ (2007) Effect of hyperoxia on cerebral metabolic rate for oxygen measured using positron emission tomography in patients with acute severe head injury. *J Neurosurg* 106:526–9

Evans AJ, Iwai F, Grist TA, Sostman HD, Hedlund LW, Spritzer CE, Negro-Vilar R, Beam CA, Pelc NJ (1993) Magnetic resonance imaging of blood flow with a phase subtraction technique. *In vitro* and *in vivo* validation. *Invest Radiol* 28:109–15

Floyd TF, Clark JM, Gelfand R, Detre JA, Ratcliffe S, Guvakov D, Lambertsen CJ, Eckenhoff RG (2003) Independent cerebral vasoconstrictive effects of hyperoxia and accompanying arterial hypocapnia at 1 ATA. *J Appl Physiol* 95:2453–61

Guyton AC, Hall JE (2005) Respiration. In *Textbook of medical physiology* (Guyton AC, Hall JE, eds), 11th edn: Saunders, Elsevier, Philadelphia

Hamberger A, Hyden H (1963) Inverse enzymatic changes in neurons and glia during increased function and hypoxia. *J Cell Biol* 16:521–5

Harik SI, Lust WD, Jones SC, Lauro KL, Pundik S, LaManna JC (1995) Brain glucose metabolism in hypobaric hypoxia. *J Appl Physiol* 79:136–40

Imray C, Booth A, Wright A, Bradwell A (2011) Acute altitude illnesses. *BMJ* 343:d4943

Jamieson D, Chance B, Cadenas E, Boveris A (1986) The relation of free radical production to hyperoxia. *Annu Rev Physiol* 48:703–19

Kety SS, Schmidt CF (1948) The effects of altered arterial tensions of carbon dioxide and oxygen on cerebral blood flow and cerebral oxygen consumption of normal young men. *J Clin Invest* 27:484–92

Kolbitsch C, Lorenz IH, Hormann C, Hinteregger M, Lockinger A, Moser PL, Kremser C, Schocke M, Felber S, Pfeiffer KP, Benzer A (2002) The influence of hyperoxia on regional cerebral blood flow (rCBF), regional cerebral blood volume (rCBV) and cerebral blood flow velocity in the middle cerebral artery (CBFVMCA) in human volunteers. *Magn Reson Imaging* 20:535–41

Liu P, Xu F, Lu H (2012) Test-retest reproducibility of a rapid method to measure brain oxygen metabolism. *Magn Reson Med*; doi:10.1002/mrm.24295 (in press)

Loeppky JA, Luft UC, Fletcher ER (1983) Quantitative description of whole blood CO2 dissociation curve and Haldane effect. *Respir Physiol* 51:167–81

Lu H, Ge Y (2008) Quantitative evaluation of oxygenation in venous vessels using T2-relaxation-under-spin-tagging MRI. *Magn Reson Med* 60:357–63

Lu H, Xu F, Grgac K, Liu P, Qin Q, van Zijl P (2012) Calibration and validation of TRUST MRI for the

estimation of cerebral blood oxygenation. *Magn Reson Med* 67:42–9
Maandag NJ, Coman D, Sanganahalli BG, Herman P, Smith AJ, Blumenfeld H, Shulman RG, Hyder F (2007) Energetics of neuronal signaling and fMRI activity. *Proc Natl Acad Sci USA* 104:20546–51
Magistretti PJ, Pellerin L (1999) Cellular mechanisms of brain energy metabolism and their relevance to functional brain imaging. *Philos Trans R Soc Lond B Biol Sci* 354:1155–63
Magnoni S, Ghisoni L, Locatelli M, Caimi M, Colombo A, Valeriani V, Stocchetti N (2003) Lack of improvement in cerebral metabolism after hyperoxia in severe head injury: a microdialysis study. *J Neurosurg* 98:952–8
Mintun MA, Raichle ME, Martin WR, Herscovitch P (1984) Brain oxygen utilization measured with O-15 radiotracers and positron emission tomography. *J Nucl Med* 25:177–87
Moller K, Paulson OB, Hornbein TF, Colier WN, Paulson AS, Roach RC, Holm S, Knudsen GM (2002) Unchanged cerebral blood flow and oxidative metabolism after acclimatization to high altitude. *J Cereb Blood Flow Metab* 22:118–26
Mudduluru M, Zubrow AB, Ashraf QM, Delivoria-Papadopoulos M, Mishra OP (2010) Tyrosine phosphorylation of apoptotic proteins during hyperoxia in mitochondria of the cerebral cortex of newborn piglets. *Neurochem Res* 35:1003–9
Nishimura N, Iwasaki K, Ogawa Y, Shibata S (2007) Oxygen administration, cerebral blood flow velocity, and dynamic cerebral autoregulation. *Aviat Space Environ Med* 78:1121–7
Nofzinger EA, Buysse DJ, Miewald JM, Meltzer CC, Price JC, Sembrat RC, Ombao H, Reynolds CF, Monk TH, Hall M, Kupfer DJ, Moore RY (2002) Human regional cerebral glucose metabolism during non-rapid eye movement sleep in relation to waking. *Brain* 125:1105–15
Noth U, Kotajima F, Deichmann R, Turner R, Corfield DR (2008) Mapping of the cerebral vascular response to hypoxia and hypercapnia using quantitative perfusion MRI at 3 T. *NMR Biomed* 21:464–72
Richards EM, Fiskum G, Rosenthal RE, Hopkins I, McKenna MC (2007) Hyperoxic reperfusion after global ischemia decreases hippocampal energy metabolism. *Stroke* 38:1578–84
Rockswold SB, Rockswold GL, Zaun DA, Zhang X, Cerra CE, Bergman TA, Liu J (2010) A prospective, randomized clinical trial to compare the effect of hyperbaric to normobaric hyperoxia on cerebral metabolism, intracranial pressure, and oxygen toxicity in severe traumatic brain injury. *J Neurosurg* 112:1080–94
Sicard KM, Duong TQ (2005) Effects of hypoxia, hyperoxia, and hypercapnia on baseline and stimulus-evoked BOLD, CBF, and CMRO2 in spontaneously breathing animals. *Neuroimage* 25:850–8
Silvennoinen MJ, Kettunen MI, Kauppinen RA (2003) Effects of hematocrit and oxygen saturation level on blood spin-lattice relaxation. *Magn Reson Med* 49:568–71
Smith ZM, Hunt JS, Li E, Guo J, Shin DD, Buxton RB, Dubowitz DJ (2011) Elevated CO2 mitigates the rise in CMRO2 during acute hypoxia and improves cerebral tissue oxygenation. In *Proceedings of the International Society for Magnetic Resonance in Medicine*. Montreal, Canada
Stein PD, Goldhaber SZ, Henry JW (1995) Alveolar-arterial oxygen gradient in the assessment of acute pulmonary embolism. *Chest* 107:139–43
Tatarkova Z, Engler I, Calkovska A, Mokra D, Drgova A, Hodas P, Lehotsky J, Dobrota D, Kaplan P (2011) Effect of long-term normobaric hyperoxia on oxidative stress in mitochondria of the Guinea pig brain. *Neurochem Res* 36:1475–81
Thom SR (2009) Oxidative stress is fundamental to hyperbaric oxygen therapy. *J Appl Physiol* 106:988–95
Tuunanen PI, Kauppinen RA (2006) Effects of oxygen saturation on BOLD and arterial spin labelling perfusion fMRI signals studied in a motor activation task. *Neuroimage* 30:102–9
Wise RG, Pattinson KT, Bulte DP, Chiarelli PA, Mayhew SD, Balanos GM, O'Connor DF, Pragnell TR, Robbins PA, Tracey I, Jezzard P (2007) Dynamic forcing of end-tidal carbon dioxide and oxygen applied to functional magnetic resonance imaging. *J Cereb Blood Flow Metab* 27:1521–32
Xu F, Ge Y, Lu H (2009) Noninvasive quantification of whole-brain cerebral metabolic rate of oxygen ($CMRO_2$) by MRI. *Magn Reson Med* 62:141–8
Xu F, Uh J, Brier MR, Hart Jr J, Yezhuvath US, Gu H, Yang Y, Lu H (2011) The influence of carbon dioxide on brain activity and metabolism in conscious humans. *J Cereb Blood Flow Metab* 31:58–67
Yezhuvath US, Lewis-Amezcua K, Varghese R, Xiao G, Lu H (2009) On the assessment of cerebrovascular reactivity using hypercapnia BOLD MRI. *NMR Biomed* 22:779–86
Zananiri FV, Jackson PC, Goddard PR, Davies ER, Wells PN (1991) An evaluation of the accuracy of flow measurements using magnetic resonance imaging (MRI). *J Med Eng Technol* 15:170–6

Supplementary Information accompanies the paper on the Journal of Cerebral Blood Flow & Metabolism website (http://www.nature.com/jcbfm)